


LARGE EDDY SIMULATION OF THE GUST INDEX OVER A REALISTIC  
URBAN AREA

(現実都市域におけるガスト指標のラージ・エディー・シミュレーション)

NURUL HUDA BINTI AHMAD



A thesis submitted in partial fulfilment of the  
requirements for the award of the degree of  
Doctor of Engineering

Department of International Development Engineering  
Graduate School of Science and Engineering  
Tokyo Institute of Technology

MARCH 2016

*A very honour dedication to my beloved  
parents, Mr. Ahmad Bin Ariffin and Mrs. Zariah Binti Che Kob,  
my supportive siblings and friends.*

## ACKNOWLEDGEMENT

In the process of completing this work, I received contributions from a number of academicians and organizations. To them, I wish to express my sincere appreciation to my supervisor, Prof. Dr. Manabu Kanda and Dr. Atsushi Inagaki for initiating this research topic and for their encouragement and guidance. Also without the support from Prof. Dr. Takayuki Aoki and Dr. Naoyuki Onodera in performing the large eddy simulation (LES) with lattice Boltzmann method (LBM), this work would not have been the same as presented. I would also like to thank the PALM group and Prof. Dr. Siegfried Raasch at the Universität Hannover for their assistance while testing the parallelized large eddy simulation model (PALM). This research could not be accomplished without the support from the Japan Society for the Promotion of Science (JSPS) KAKENHI Grant Numbers 25249066 and 26420492 and the support received from the Joint Usage/Research Center for Interdisciplinary Large-scale Information Infrastructures and High performance Computing Infrastructure in Japan. I am also indebted to the Ministry of Higher Education (MOHE) for granting me sponsorships (SLAI) and to the Universiti Teknologi Malaysia (UTM) for approving my study leave. The Tokyo Tech's librarians also deserved special thanks for their assistance in supplying me with some relevant materials and data. I extend my sincere appreciation to all Kanda Lab's members especially to Dr. Alvin Christopher Galang Varquez and Miss Ayako Yagi, not to forget, Mrs. Yuko Okamoto for their supports and assistance since the beginning of this work. I am grateful to many Malaysian and international colleagues for their comments at different stages of this work. Finally, my gratitude is due to my parents and family members for their sacrifices, concerns and undying love.

## ABSTRACT

The aim of this research is to quantitatively present a general relationship between the intensity of gusts and the urban morphology. Two large eddy simulation (LES) models named as the parallelized LES model (PALM) and lattice Boltzmann model (LBM) were executed. It was confirmed that both models produce the same accuracy. The PALM was used to validate the new gust parameter while the LBM was applied to simulate and examine the gusts environment without uncertainties in the inflow condition. The coastal area of Tokyo was selected to represent the urban morphology. The simulations run over realistic geometry surfaces of the build up area with 2 m resolution in all direction to explicitly resolve the fine building shape and also the flow at the pedestrian level. It considers only the shear driven turbulence (i.e. no Coriolis force and thermal stratification) and developed the boundary layer naturally. A new parameter called the gust index (GI) was defined as the local maximum wind speed divided by the free stream velocity. This universalize definition make it comparable quantitatively at different locations within urban canopies. Moreover, this parameter is decomposed into mean wind ratio (MWR) and turbulent part ratio (TPR) component to evaluate the quality of gustiness. This procedure can mask detailed structures of individual buildings with keeping the bulk characteristics of the urban morphology. At the pedestrian level, it is quantitatively shown that the GI decrease with increasing building coverage,  $\lambda_p$ , which notably contribute by the TPR through out the range of  $\lambda_p$  compared to the MWR. Such a result was explained by the change of flow regimes within the building canyon. Apparently, at the higher elevation above the canopy layer, the effect of the building coverage becomes irrelevant to all normalized velocity ratios and the roughness length, as a comprehensive aerodynamic property of roughness was well represented.

## SUMMARY (JAPANESE)

本論は「Large Eddy Simulation of the Gust Index over a Realistic Urban Area」（現実都市域におけるガスト指標のラージ・エディター・シミュレーション）と題して、英文で書かれ、以下の 8 章から構成される。

第 1 章「Introduction」（序論）では、おもに風工学分野と気象学分野で行われてきた従来のガストに関するレビューを行い、ガストの定義方法、歩行高さにおける平均風速などの旧来の成果について問題点・研究課題を提示し、本論の動機・目的について論じている。

第 2 章「Description of an Appropriate Spatial Gust Index」（適切な空間ガスト指標について）では突風現象の定量評価のためのガスト指標（gust index）を提案した。従来の突風率（gust factor）は最大風速と局所的な時間平均値の比として定義され、街区の淀み域でも大きな値をとりうる。これに対し外層風速との比と定義することで、突風の強さを 1 次元的に評価することができる。これにより街区内での場所の比較のみならず、サイト間の比較なども可能となる。

第 3 章「Description of the simulation model」（シミュレーションモデルについて）では、本研究で使用した格子ボルツマン法 LES モデル及び、Navier-Stokes 方程式に基づく LES モデルの方程式系について記述した。また、計算対象領域である東京都臨海部の建物分布について記した。

第 4 章「Validation」（モデル評価）では、格子ボルツマン法 LES のモデル性能評価を目的とし、風洞実験及び使用実績豊富な Navier-Stokes 式に基づく LES モデルとの比較を行い、両モデルがほぼ同程度の精度を持つこと

を明らかにした。また、ガスト指標の外力(外層風速)依存性について検討するため、実都市幾何形状を地表面に配した気流のシミュレーションを行い、大気境界層の現実的な外層風速の範囲内では、ガスト指標が外力に依存しないことを示した。

第5章「General description of the flow field within a realistic urban area」(現実都市域における流れの性質)では、基本的な乱流統計量の性質について記述した。風洞実験における粗面及び滑面の乱流境界層との比較を行った結果、地表面近傍では違いが出るものの、境界層高度の約半分以上では地表面性状に依らない乱流統計量の相似性が概ね成り立つことを示した。

第6章「Horizontal distribution of the flow field within a realistic urban area」(現実都市域における流れ場の水平分布構造)では、瞬間及び平均風速、レイノルズ応力の水平断面分布を描画し、地物の影響範囲について検討を行った。ガスト指標の空間分布を描画し、これについても地物との対応関係を視覚的に示した。

第7章「General relationship between the gust index and the urban morphology」(ガスト指標と都市幾何形状の普遍的な関係)では、ガスト指標と建物分布との関係性について議論した。計算領域を水平方向の小領域に分割し、その小領域の中でガスト指標の平均値及び、マクロな建物幾何パラメータ(平均建物高さや建蔽率)を算出し、比較した。これにより歩行者レベルのガスト指標が建蔽率に対してほぼ線形に減少することを明らかにした。また、その勾配がある建蔽率を境に大きく変わることが分かり、これは従来提案されている2次元建物キャノピーの流れ分類で説明できることを示した。

第8章「Concluding remarks」(結論)では本研究成果及び、現時点で未解決の点を記述した。

以上要するに、本論文は数値計算に基づく実都市の突風評価手法を提案するものであり、都市気象・都市計画分野で工学上高く評価される。よって、博士(工学)として価値が十分あるものと認められる。

## TABLE OF CONTENTS

<b>CHAPTER</b>	<b>TITLE</b>	<b>PAGE</b>
	<b>DECLARATION</b>	ii
	<b>DEDICATION</b>	iv
	<b>ACKNOWLEDGEMENT</b>	v
	<b>ABSTRACT</b>	vi
	<b>SUMMARY (JAPANESE)</b>	vii
	<b>TABLE OF CONTENTS</b>	ix
	<b>LIST OF FIGURES</b>	xii
	<b>LIST OF SYMBOLS</b>	xvii
	<b>LIST OF APPENDICES</b>	xx
	<b>LIST OF TABLES</b>	xxii
<b>1</b>	<b>INTRODUCTION</b>	<b>1</b>
	1.1 Literature Review	1
	1.1.1 General gusts definition	1
	1.1.2 Urban surface geometry and wind environment at the pedestrian level	3
	1.1.3 Mean wind velocity ratio at the pedestrian level	4
	1.1.4 Gusts at the pedestrian level	5
	1.1.5 General meteorological studies of gusts	6
	1.2 Background of the Research Problem	7
	1.3 Objective and Importance of the Study	8
	1.4 Scopes of the Study	9
	1.5 Summary	10

<b>2</b>	<b>DEFINING AN APPROPRIATE SPATIAL GUST INDEX</b>	<b>12</b>
	2.1 Introduction	12
	2.2 The Spatial Gust Index	13
	2.3 The Gust Index and its Component	14
	2.4 Summary	15
<b>3</b>	<b>DESCRIPTION OF THE SIMULATION MODEL</b>	<b>16</b>
	3.1 Introduction	16
	3.2 Parallelized Large Eddy Simulation Model	17
	3.2.1 Model description	17
	3.2.2 Simulation setup	19
	3.3 Lattice Boltzmann Method and Large Eddy Simulation	20
	3.3.1 Model description	20
	3.3.2 Simulation setup	23
	3.4 Summary	25
<b>4</b>	<b>VALIDATION</b>	<b>26</b>
	4.1 Introduction	26
	4.2 Simulation Models Inter-comparison	27
	4.3 Justification of the Gust Index Definition	30
	4.4 Summary	31
<b>5</b>	<b>GENERAL DESCRIPTION OF THE FLOW FIELD WITHIN A REALISTIC URBAN AREA</b>	<b>32</b>
	5.1 Introduction	32
	5.2 Urban Geometry Parameters and Boundary Layer Development	33
	5.3 Wind Flow Properties	36
	5.3.1 Streamwise profile	36
	5.3.2 Vertical profile	37
	5.4 Summary	38



<b>6</b>	<b>HORIZONTAL DISTRIBUTION OF THE FLOW FIELD WITHIN A REALISTIC URBAN AREA</b>	<b>39</b>
6.1	Introduction	39
6.2	Horizontal Distribution of the Flow Field	40
6.2.1	Instantaneous wind velocity	40
6.2.2	Mean wind velocity	41
6.2.3	Reynolds stress	41
6.2.4	Standard deviation	42
6.3	Horizontal Distribution of the Gust Index and its Component	54
6.4	Summary	58
<b>7</b>	<b>GENERAL RELATIONSHIP BETWEEN THE GUST INDEX AND THE URBAN MORPHOLOGY</b>	<b>59</b>
7.1	Introduction	59
7.2	Determination of the Optimum Size of Patches	60
7.3	Influence of Boundary Layer Development on the Normalised Velocity Ratios	63
7.4	General Relationship between Pedestrian-level Flow Characteristics and the Plan Area Index	67
7.5	The Gust Index and its Component at Different Heights	70
7.6	Summary	73
<b>8</b>	<b>CONCLUDING REMARKS</b>	<b>75</b>
8.1	Introduction	75
8.2	Research Findings	76
8.3	Recommendations and Implications for Further Research	77
8.4	Summary	78
	<b>REFERENCES</b>	<b>79</b>
	<b>APPENDICES</b>	<b>83</b>

## LIST OF FIGURES

FIGURE NO.	CAPTION	PAGE
1.1	Gusts in an urban area, illustration taken from the Classification Table of the Rain and Wind leaflet, JMA (2014).	4
1.2	Research flowchart	11
3.1	Building height distribution of the (a) commercial land (b) skyscrapers (c) residential area.	19
3.2	The arrows represent the directions of the fluid populations (i.e., a set of 18 discrete velocities including one null vector corresponding to particles at rest) according to the D3Q19 scheme Bernaschi et al. (2010).	21
3.3	Three dimensional scaled view of the building height data.	24
3.4	Building height within 19.2 km ( $X$ ) $\times$ 4.8 km ( $Y$ ) $\times$ 1 km ( $Z$ ) simulation domain of an urban area of Tokyo.	24
4.1	Domain setting for the validation simulation. Red lines show each measurement location ( $x/H = -1, 0, 0.5, 1, 1.5, 2.5$ ).	27
4.2	Vertical profile of the average wind speed, $U$ , normalized to the bulk inflow cross-section average wind speed, $U_b$ . Experiment data shown by the dotted line. Each profile represents the position mentioned in Fig. 2.3.	28

4.3	The streamlines around the cube centre vertical cross-section and lowermost horizontal cross-sectional. N is the number of grids to resolve the cube piece.	28
4.4	Comparison between the PALM and LBM-LES vertical profile of $U/U_b$ . Domain resolution of (a) 3 m (N=16), (b) 1.5 m (N=32) and (c) 0.75 m (N=64) is homogeneous in all direction ( $dx=dy=dz$ ).	29
4.5	Probability density distribution of the (i) maximum wind speed, $U_{max}$ and for four different definitions of the gust index, (ii) $U_{max}/U_{ave}$ , (iii) $U_{max}/U^*$ , (iv) $U_{max}/U_{loc}$ , (v) $U_{max}/U_{\infty}$ for the (a) commercial land (b) skyscrapers (c) residential area.	30
5.1	Geometry parameter of the simulation domain. (a) Maximum building height, $H_{max}$ , average building height, $H_{ave}$ and its standard deviation $\sigma_H$ . (b) The plan area index, $\lambda_p$ and frontal area index, $\lambda_f$ .	34
5.2	Boundary layer height, $\delta$ calculated from the (a) simulation and compared with (b) Garratt 1989. (c) Normalised values of the $H_{ave}$ and $\sigma_H$ to the $\delta$ .	35
5.3	The friction velocity, $u_*$ , freestream velocity, $U_{\infty}$ and the normalised boundary layer height along the domain streamwise, $d\delta/dx$ .	36
5.4	Profiles against $z/\delta$ of (a) $U/u_*$ , (b) $\overline{u'w'}/u_*^2$ , (c) $\sigma_u/u_*$ , (d) $\sigma_v/u_*$ and (e) $\sigma_w/u_*$ .	37
6.1	Horizontal distribution ( $xy$ -plan) of the instantaneous wind velocity, $u_{ins}$ , at 2, 54, 98 and 198 m height.	43
6.2	Horizontal distribution ( $xy$ -plan) of the mean wind velocity ( $u$ -component) at 2, 54, 98 and 198 m height.	44
6.3	Horizontal distribution ( $xy$ -plan) of the mean wind velocity ( $v$ -component) at 2, 54, 98 and 198 m height.	45
6.4	Horizontal distribution ( $xy$ -plan) of the mean wind velocity ( $w$ -component) at 2, 54, 98 and 198 m height.	46

6.5	Horizontal distribution ( <i>xy</i> -plan) of the Reynolds stress (instantaneous component) at 2, 54, 98 and 198 m height.	47
6.6	Horizontal distribution ( <i>xy</i> -plan) of the Reynolds stress (mean component) at 2, 54, 98 and 198 m height.	48
6.7	Horizontal distribution ( <i>xy</i> -plan) of the Reynolds stress (turbulent component) at 2, 54, 98 and 198 m height.	49
6.8	Horizontal distribution ( <i>xy</i> -plan) of the standard deviation ( <i>v</i> -component) at 2, 54, 98 and 198 m height.	50
6.9	Horizontal distribution ( <i>xy</i> -plan) of the mean wind velocity ( <i>v</i> -component) at 2, 54, 98 and 198 m height (same as Fig. 6.3 but following the colour range of Fig. 6.8).	51
6.10	Horizontal distribution ( <i>xy</i> -plan) of the standard deviation ( <i>w</i> -component) at 2, 54, 98 and 198 m height.	52
6.11	Horizontal distribution ( <i>xy</i> -plan) of the mean wind velocity ( <i>w</i> -component) at 2, 54, 98 and 198 m height (same as Fig. 6.4 but following the colour range of Fig. 6.10).	53
6.12	Gust index distribution at 2 m height for the 1,000 m × 1,000 m of the (a) commercial land, (b) skyscrapers and (c) residential area by using the proposed definition.	54
6.13	Horizontal distribution of the (a) gust index, $\tilde{U}_{max}$ , (b) mean wind ratio, $\tilde{U}$ , and (c) turbulent part ratio, $\tilde{U}'$ , at 2 m height.	55
6.14	Magnified view overlain with the building height of the (a) gust index, $\tilde{U}_{max}$ , (c) mean wind ratio, $\tilde{U}$ , (d) turbulent part ratio, $\tilde{U}'$ , from Fig. 5.3 and (b) the spatial distribution of the conventional gust factor, $G$ .	57
7.1	The bin analysis of the spatial average of the different patch sizes of the (a) gust index, $[\tilde{U}_{max}]_{\lambda_p bin}$ , (b) mean wind speed ratio, $[\tilde{U}]_{\lambda_p bin}$ , and (c) turbulent part ratio, $[\tilde{U}']_{\lambda_p bin}$ , versus the plan area index, $[\lambda_p]_{bin}$ , at 2 m height for the latter half of the simulation domain.	61

- 7.2 Standard deviation bias analysis of the different patch sizes ( $m^2$ ) from the gust index,  $[\tilde{U}_{max}]_{\lambda_p bin}$ , mean wind speed ratio,  $[\tilde{U}]_{\lambda_p bin}$ , and turbulent part ratio,  $[\tilde{U}']_{\lambda_p bin}$ . 62
- 7.3 The boundary layer development along streamwise,  $x$ . Also shown the quarters distance from the domain inlet (Q1) to the outlet (Q4). 63
- 7.4 The spatial and bin average of the  $480 \times 480 m^2$  patches for the gust index,  $[\tilde{U}_{max}]_{\lambda_p bin}$ , mean wind speed ratio  $[\tilde{U}]_{\lambda_p bin}$ , and turbulent part ratio,  $[\tilde{U}']_{\lambda_p bin}$  versus the plan area index,  $[\lambda_p]_{bin}$ , at 2 m for the whole domain divided into four quarter in the streamwise direction. 64
- 7.5 The spatial average of the  $480 \times 480 m^2$  patches for The gust index,  $[\tilde{U}_{max}]$  versus the plan area index,  $\lambda_p$ , at 2 m for the last three quarters (Q2+Q3+Q4). Chosen isolated scatter plots (red circle) and closed to linear trendline (green circle) were  $0.415 < \lambda_p < 0.432$ . 66
- 7.6 Selected  $480 \times 480 m^2$  patches of Fig. 7.5 and its corresponding plan area index,  $\lambda_p$  and gust index,  $[\tilde{U}_{max}]$ . Isolated scatter plot (Patch 15, 91 and 330) and closed to linear trendline (others). 66
- 7.7 The spatial and bin average of the  $480 \times 480 m^2$  patches for the gust index,  $[\tilde{U}_{max}]_{\lambda_p bin}$ , mean wind speed ratio,  $[\tilde{U}]_{\lambda_p bin}$ , and turbulent part ratio,  $[\tilde{U}']_{\lambda_p bin}$ , versus the plan area index,  $[\lambda_p]_{bin}$ , at 2 m for the last three quarters from the domain inlet (Q2 + Q3 + Q4) and the latter of the half domain (Q3 + Q4). 68
- 7.8 Same as Fig. 7.5 but only for the latter half domain (Q3+Q4). 71

- 7.9 Selected  $480 \times 480 \text{ m}^2$  patches of Fig. 7.8 and its corresponding plan area index,  $\lambda_p$  and gust index,  $[\tilde{U}_{max}]$ . Isolated scatter plot (Patch 21, 23, 260, 300, 318 and 381) and closed to linear trendline (others). 71
- 7.10 The gust index,  $[\tilde{U}_{max}]$ , mean wind speed ratio,  $[\tilde{U}]$ , and turbulent part ratio,  $[\tilde{U}']$ , versus the plan area index,  $[\lambda_p]$ , and the roughness length,  $[z_0]$  in the  $480 \times 480 \text{ m}^2$  patches at a height of 2 and 16 m for the latter half of the domain (Q3 + Q4). 72

## LIST OF SYMBOLS

$A$	-	Area/Sample	$m^2$
$C$	-	Model coefficient	
$c$	-	Velocity vector	
$dx$	-	Grid length in $x$ -direction	$m$
$dy$	-	Grid length in $y$ -direction	$m$
$dz$	-	Grid length in $z$ -direction	$m$
$E$	-	Magnitude of the velocity gradient tensor	
$g$	-	Gravitational force	$m\ s^{-2}$
$k$	-	Turbulence kinetic energy	$m^2\ s^{-2}$
$k$	-	Height of the roughness element	$m$
$m$	-	Gradient	
$N$	-	Grid resolution	
$n$	-	Total number of sample	
$Q$	-	Velocity gradient tensor	
$q$	-	Specific humidity	
$t$	-	Time	$s$
$H$	-	Cube/building height	$m$
$U$	-	Mean wind speed	$m\ s^{-1}$
$\tilde{U}$	-	Mean wind ratio	
$\tilde{U}_{max}$	-	Gust index	
$\tilde{U}'$	-	Turbulent part ratio	
$u$	-	Wind velocity in streamwise ( $x$ -direction)	$m\ s^{-1}$
$uw$	-	Reynolds stress (mean component)	$m^2\ s^{-2}$
$v$	-	Wind velocity in spanwise ( $y$ -direction)	$m\ s^{-1}$
$w$	-	Wind velocity in vertical direction ( $z$ -direction)	$m\ s^{-1}$
$X, x$	-	Computation domain streamwise ( $x$ -direction)	$m$
$Y, y$	-	Computation domain spanwise ( $y$ -direction)	$m$

$Z, z$	-	Computation domain height ( $z$ -direction)	m
$z_0$	-	Roughness length	m
$\delta$	-	Boundary layer height	m
$\varepsilon$	-	Turbulence dissipation	$\text{m}^2 \text{s}^{-3}$
$\lambda$	-	Area index	
$\Delta$	-	Interval/width	
$\nu$	-	Kinematic viscosity	$\text{m}^2 \text{s}^{-1}$
$\omega$	-	Weighting factor	
$\rho$	-	Density	$\text{kg m}^3$
$\tau$	-	Relaxation time	s
$\sigma$	-	Standard deviation	m
$\theta$	-	Potential temperature	K
$[ \ ]$	-	Values average in patch size	
$[ \ ]_{bin}$	-	Values average in bin range	

#### Superscript/Subscript/Accent

<i>ave</i>	-	Average
<i>b</i>	-	Bulk
<i>f</i>	-	Frontal
<i>i</i>	-	$i$ -th number of sample
<i>ins</i>	-	Instantaneous
<i>loc</i>	-	Local
<i>max</i>	-	Maximum
<i>p</i>	-	Plan
$\infty$	-	Freestream
*	-	Friction
'	-	Turbulent
~	-	Ratio



- - Mean
- 1, 2, ... - Assigned number for the reference/point

#### Abbreviation

- ABL - Atmospheric boundary layer
- BGK - Bhatnagar-Gross-Krook
- CAD - Computer-aided design
- CFD - Computational fluid dynamics
- CS - Coherent-structure
- CSM - Coherent-structure Smagorinsky model
- D3Q19 - Three dimensional, 18 discrete velocities (plus one null)
- GI - Gust index
- GPU - Graphics processing units
- GS - Grid scale
- IMUK - Institute of Meteorology and Climatology
- JMA - Japan Meteorological Agency
- LBM - Lattice Boltzmann method
- LES - Large eddy simulation
- MOST - Monin-Obukhov similarity theory
- MWR - Mean wind ratio
- NOAA - National Oceanic and Atmospheric Administration
- PALM - Parallelized LES model
- Q - Quarter
- SGS - Subgrid-scale
- TKE - Turbulent kinetic energy
- TPR - Turbulent part ratio

## LIST OF APPENDICES

APPENDIX	TITLE	PAGE
A1	Tokyo meteorological station, retrieved from Japan Meteorological Agency (JMA).	84
A2	Tokyo wind yearly wind measurement, retrieved from Japan Meteorological Agency (JMA).	85
A3	Tokyo wind monthly wind measurement, retrieved from Japan Meteorological Agency (JMA).	86
A4	Tokyo wind daily wind measurement, retrieved from Japan Meteorological Agency (JMA).	87
A5	Tokyo wind 10 min wind measurement, retrieved from Japan Meteorological Agency (JMA).	88
A6	リーフレット「雨と風（雨と風の階級表）」 [Leaflet "Rain and wind (Class tables of rain and wind)"], retrieved from Japan Meteorological Agency (JMA).	89
A7	Comparing the streaky pattern of the instantaneous wind speed, $u_{ins}$ from the LES-LBM simulation and the Doppler lidar observation.	90
A8	Decomposition of the whole domain into 400 patches ( $480 \times 480 \text{ m}^2$ for each patch).	91
A9	Program to determine the ‘kink’ point by using multi-phase linear regression and least mean square method (run using Python).	92

A10 'Kink' point for the mean wind ratio,  $[\tilde{U}]$ , and the turbulent part ratio,  $[\tilde{U}']$ , versus the plan area index,  $\lambda_p$ . Spatial average distribution of the  $480 \times 480 \text{ m}^2$  patches for the last three quarters (Q2+Q3+Q4).

93

## LIST OF TABLES

TABLE	TITLE	PAGE
1.1	The strength of the wind blow, translated from the Classification Table of the Rain and Wind leaflet, JMA (2014).	2
1.2	Summary of gust factors, Davis and Newstein (1968).	7
7.1	The gradient, $m$ , of the mean wind speed ratio, $[\tilde{U}]$ , and the turbulent part ratio, $[\tilde{U}']$ , of the plan area index $[\lambda_p] < 0.28$ and $[\lambda_p] > 0.28$ from selected patches of Fig 7.7	68

## **CHAPTER 1**

### **INTRODUCTION**

#### **1.1 Literature Review**

##### **1.1.1 General gusts definition**

The National Oceanic and Atmospheric Administration (NOAA) defined the gusts as a sudden, brief increase wind speed above the average wind speed. Based on the U.S. weather observing practice, the wind speed is qualify as gusts when the maximum wind speed reaches at least  $30 \text{ km h}^{-1}$ , deviate between the peaks and calm condition at about  $17 \text{ km h}^{-1}$  and lasting for less than 20 s. The Editors of Encyclopaedia Britannica added that gusts cause by the turbulent flow around an obstacle which occur regularly over buildings and rough ground. From these definitions, gusts can generally describe as the disturbed air that blown in sudden, high speed and in a short period of time and it potentially gave an impact on its surrounding. In getting more clear understanding on the physical meaning of the strength of the blown wind, the Japan Meteorological Agency (JMA) categorized the wind speed and it effect towards the pedestrian, vegetation, moving car and the infrastructure as summarized in Table 1.1.

**Table 1.1** The strength of the wind blow, translated from the Classification Table of the Rain and Wind leaflet, JMA (2014).

	Average wind speed (m s <sup>-1</sup> )	Approximate wind speed (km h <sup>-1</sup> )	Forecast terminology	Indication of speed	Pedestrian	Vegetation and utility	On road transportation	Building and infrastructure	Instantaneous wind speed (m s <sup>-1</sup> )
Wind advisory	10~15	~50	Somehow strong wind	On road transportation speed	It is difficult to walk against the wind.	Whole trees and wires begin to sway.	Feel the crosswind if the the transport in the high speed and the wind stream perpendicular to it.	The antenna begins to sway.	20
	15~20	~70	Strong wind		Walk against the wind will cause fall. Work at high level is extremely dangerous.	Wire, signboards and galvanized iron plate begins to flutter.	During the high-speed operation, the driver can sense the increase in the crosswind.	The roof, tiles, roofing material peeled off. Shutters start to shake.	
High wind warning	20~25	~90	Very strong wind	Highway transportation speed	Need to hold on to something to stand. Fear to be injured by the flying objects.	Broken tree or thin trunk and trees that do not have a strong roots grip begin to collapse. Signboards fall and scattered. Road signs tilt.	It becomes difficult to drive at a normal speed.	The roof, tiles, roofing material scattered.	30
	25~30	~110							
Extreme wind warning	30~35	~125	Severe wind	Express train	Outdoor condition is very dangerous.	Many of the trees, poles and street lights fall. Block wall collapsed.	The wind able to rollover a moving truck.	Inadequate metal roof or temporary scaffolding starts to collapse.	40
	35~40	~140						Exterior materials are scattered over a wide range, which exposed the base material.	
	40~	140~						May collapse a living house. May cause deformed in the steel structure.	

Wind advisory
  High wind warning
  Extreme wind warning

The JMA averaged the wind speed within 10 min, while the instantaneous wind speed duration is of 3 s. Referring to Table 1.1, the instantaneous wind speed is about 1.5 times the average wind speed. The wind was measured based on the unstable atmospheric conditions. The wind speed phenomenon at a certain location and its consequence damage as described in the table may significantly differ from the nearby observation measurement due to the terrain and surrounding buildings. Although the wind speed is the same, the state of damage is different depending on the blowing way of the wind and the structure affected.

Gusts term might easily misunderstood as this phenomenon dependence on many factor such as its scale, source, location of occurrence, etc. Therefore, gusts were reviewed in several sections in this chapter as following.

### **1.1.2 Urban surface geometry and wind environment at the pedestrian level**

It is vital to understand the wind flows close to the ground in densely built up areas because most activities of the residents occur at this level. Anomalous and unpredictable gusts may occur when wind flows through the maze created by a rugged urban landscape. Pedestrians and infrastructure may be harmed from such gusts, including injuries, death, damage, destruction of urban vegetation, power outages and traffic collisions as illustrated in Fig. 1.1. These negative impacts of gusts have encouraged the comprehensive study of the complex flows found within large urban areas and attempts to determine their relationships with the urban morphology.

This research empirically relate gusts at the pedestrian level with “bulk” geometrical parameters at the district or city scale, thereby identifying high-risk areas for gusts in terms of various urban morphologies.



**Figure 1.1** Gusts in an urban area, illustration taken from the Classification Table of the Rain and Wind leaflet, JMA (2014).

### 1.1.3 Mean wind velocity ratio at the pedestrian level

The flow environment should be evaluated in terms not only of the gusty flow but also of the mean flow. In addition, since the concept to analyse the mean wind environment is useful also for analysing the gusty flow, the conventional studies on the mean wind ratio are reviewed.

Some studies have attempted to predict spatially averaged mean velocity profiles within urban canopies using simple models (Macdonald 2000; Martilli et al. 2002; Coceal and Belcher 2004). Although these models are very useful for approximately determining the mean wind profile within the canopy layer, they cannot precisely predict the mean wind velocity close to the ground, as demonstrated by a direct numerical simulation (Leonardi and Castro 2010). Moreover, these models are mostly validated for homogeneous building arrays rather than more realistic complicated building arrangements.

Some studies have examined the wind environment in cities at the pedestrian level in terms of the mean wind ratio (MWR), which is defined as the mean wind



speed ( $U$ ) normalised by the free stream velocity ( $U_\infty$ ). [Kubota et al. \(2008\)](#) conducted a wind tunnel test using scaled models of selected detached and apartment houses from real cities in Japan. They reported that the MWR decreases in areas with higher plan area index ( $\lambda_p$ ) values. [Hu and Yoshie \(2013\)](#) used a computational fluid dynamics (CFDs) turbulence model as a reference urban model of a typical residential area in Shanghai, and found that the MWR was affected not only by  $\lambda_p$  but also by the configuration of roughness in urban areas, variation in the heights of buildings, and wind direction. A large eddy simulation (LES) by [Razak et al. \(2013\)](#) for simplified but varied building arrays demonstrated a robust relationship in which the MWR decreased with an increase in the frontal area index ( $\lambda_f$ ). Taken together, these studies suggest the possibility that the MWR can be explained by simple geometrical indices such as  $\lambda_p$  and  $\lambda_f$ .

In this research, the similar approach was followed for the gusts. In addition, the MWR in the urban area is also evaluated.

#### **1.1.4 Gusts at the pedestrian level**

Researchers in the fields of wind engineering and architectural engineering have investigated gusts at the pedestrian level. The main focus has been on detailed and local flow structures around a single building or specific building clusters rather than on the overall relationship between gusts and bulk geometrical parameters at the district or city scale. [Murakami et al. \(1983\)](#) conducted a long-term observation of gusts around a single high-rise building and its surroundings near the surface. The large amount of data collected was analysed to make a detailed estimate of the local gust factor distribution around buildings. [He and Song \(1999\)](#) performed an LES to simulate the wind flow at 2 m above the ground around a group of buildings with different geometries. The gusts associated with different wind conditions were visualised in detail.

Recent developments in computational resources have allowed computations of town-scale urban airflows at high spatial resolution. Some studies have examined the effects of not only individual buildings but also groups of buildings on street-level flows. These studies conducted simulations of turbulent flow in and above cubical roughness, and revealed that turbulent organized structures are much larger than surface obstacles (Kanda et al. 2004; Kanda 2006; Castillo et al. 2011). Moreover, Inagaki et al. (2012) demonstrated that such turbulent structures predominantly determine the instantaneous flow distribution within the canopy layer. Park et al. (2013) simulated turbulent flow in an actual city with a 5 m domain resolution, and observed a tail-off in the coherent turbulent structure induced by significantly tall buildings at a great distance downstream. However, it has proven difficult to obtain a general and quantitative description of gusts at the pedestrian level and to understand their relationships with the urban morphology. This is probably due to the complexity of the building morphology, together with the three-dimensionality and intermittent nature of turbulence.

### 1.1.5 General meteorological studies of gusts

Most gust studies have been conducted within the framework of conventional meteorology, including the definition of gusts, the time required to define the average and/or maximum wind velocity, the statistical features of gusts, and the influential meteorological parameters of gusts (e.g., surface roughness, observation height, atmospheric stability, etc.). Such studies have not focused on the pedestrian level but rather on the surface layer based on Monin-Obukhov Similarity Theory (MOST) (Monahan and Armendariz 1971; Wieringa 1973; Wilson 2000; Verkaik 2000; Azad and Alam 2010).

The gustiness that summarized in Table 1.2, is the normalized values of the maximum wind speed by the mean wind speed. The averaging time for the mean wind speed and the interval of the maximum wind speed varies between each investigator. The factors will be lower as the maximum wind speed duration is shorter and/or the greater the mean wind speed averaging time. In term of different in

the measurement height (not shown in the table), [Davis and Newstein \(1968\)](#) suggested that the gust factor should decrease with height by referring the assembled data from many investigators.

**Table 1.2** Summary of gust factors, [Davis and Newstein \(1968\)](#).

Investigator	Range of gust factor	Time average of mean wind speed	Duration of maximum wind speed
Brekker (1959)	1.30-1.08	varies	-
Cramer (1960)	1.62-1.38	10 min	instantaneous
Deese (1964)	2.00-1.20	5 min	instantaneous
Durst (1960)	1.59-1.00	1 h	1 h to 0.5 s
Faber and Bell (1963)	2.05-1.28	1 h	Instantaneous to 1 min
Shellard (1965)	1.90-1.30	10 min	3-5 s
Vellozzi and Cohen (1967)	1.56	1 h	1 s

Due to the locality of the urban area, several parameters especially the mean wind speed change by points and locations mainly wind flow at the pedestrian level. Therefore, this conventional approach needs to be modified to make it universal and comparable with other locations or even experiments.

## 1.2 Background of the Research Problem

A vigorous and populous urban landscape might be vulnerable in the unpleasant wind event such as a strong gust. As a consequence of this fact, it is essential to understand the features of the wind flow within this area particularly at the pedestrian level. As reviewed above, there are so many studies related to the wind flow and/or gust at different scale. The micro- and local-scale studies might focus on the pedestrian level which consider only a single building ([Murakami et al. 1983](#)), a cluster of real building ([He and Song 1999](#)), simplified urban model ([Hu and Yoshie 2013](#), [Razak et al. 2013](#), [Inagaki et al. 2012](#)) or even the real urban area ([Kubota et al. 2008](#), [Park et al. 2013](#)). It is capable to map the spatial distributions of

the wind statistics for these studies. For a bigger scale (i.e., meso-scale), the wind and/gust measured at a surface layer level at a certain location (i.e., point measurement).

It is discovered that there is lacking in understanding the gust that occur in an acceptable huge area horizontally which comprise a realistic urban roughness. Moreover, the relationship between the flow characteristics in the surface layer and those at the pedestrian level (Sect. 7.5 of Chapter 7) are not reveal yet by the previous researcher. Thus, it is suggested that there are some gaps between the results from studies undertaken in the two disciplines in which gusts are commonly studied: wind engineering (Sect. 1.1.4) and meteorology (Sect. 1.1.5).

### **1.3 Objective and Importance of the Study**

Although the researches on gusts are many, those matching the purpose of this research are rare as reviewed in the previous sections.

Thus, this research is important to reveal the wind flow characteristics specifically the gusts within this build up area and determine a general similarity and description that can associate the different scale or level as mentioned before. It can be done by assigning an appropriate definition for the related parameter.

Furthermore, this research was highly motivated by a simulation of the wind flow over a huge urban area performed by [Onodera et al. \(2013\)](#). Therefore, it is feasible to achieve the final goal of this study which is to quantitatively analyse the relationship between the gust at the urban pedestrian levels and the building morphology.

## 1.4 Scopes of the Study

The ultimate objective of this study was achieved by coordinating the research framework as shown in Fig. 1.2. This structured workflow is elaborated in the sequential chapters. The basic understanding on gusts is reviewed in the previous section of this chapter. The conventional gust factor and proposed spatial gust index are defined in Chapter 2. Next, Chapter 3 describes the large eddy simulation (LES) models which executed mainly to resolve the instantaneous wind speed and other wind flow elements within a realistic city. The preliminary study contributes in defining an appropriate spatial gust index performed by parallelized LES model (PALM). Subsequently, the lattice Boltzmann method (LBM) was conducted to reach the main purpose of this research. Both LES models were validated and demonstrated in Chapter 4. In stead of that, the gust index defined in Chapter 2 is also justified in this chapter. Following, Chapter 5 and 6 presents the general description of the flow field by the wind profile (in the streamwise and vertical direction and the related geometrical parameters) and horizontal distribution (including the spatial gust index map) respectively; focusing on the statistics computed from the LBM simulation. The foremost part of this research as priory mentioned (Sect. 1.2) contributes in Chapter 7. Finally, the concluding remarks and several recommendations for future work are stated in Chapter 8.

## 1.5 Summary

In a nutshell, this chapter introduced and reviewed the wind environment in the urban area specifically the gust at the pedestrian level. A clear objective in finding the general relation between the gust index and the urban morphology empirically was stated. The general overview of the research was also described for the following chapters. It is expected that this study will contribute some knowledge about the gust in an urban area and also fill some gap between the two streams of the gust studies which are the wind engineering and the meteorology.

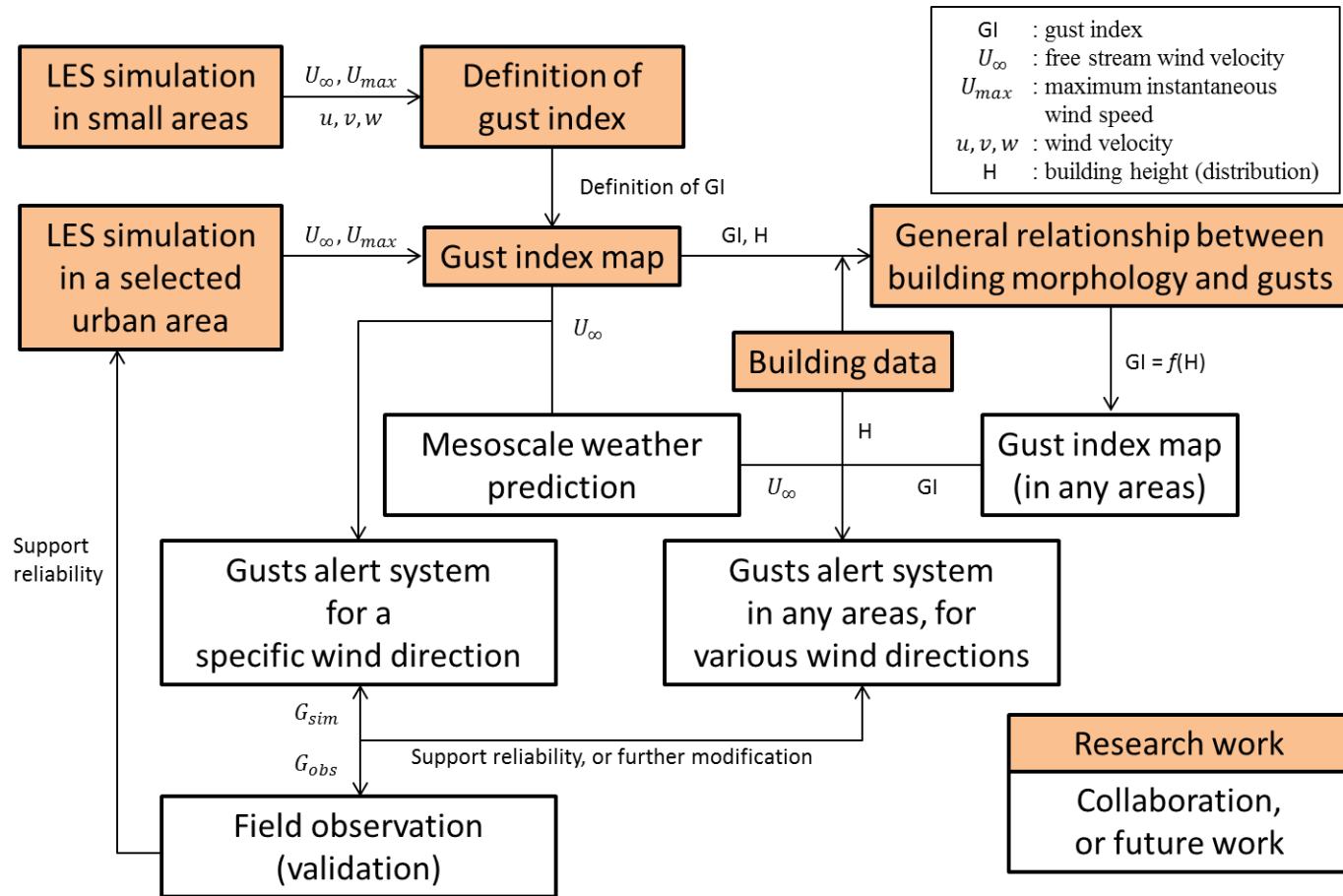


Figure 1.2 Research flowchart.

## REFERENCES

- Azad AK, Alam MM (2010) Determination of Wind Gust Factor at Windy Areas of Bangladesh. In 13th Asian Congress of Fluid Mechanics, 17-21 December, 2010, IUT, Dhaka, Bangladesh, pp 521-524
- Bernaschi M, Fatica M, Melchionna S, Succi S, Kaxiras E (2010) A flexible high-performance Lattice Boltzmann GPU code for the simulations of fluid flows in complex geometries. *Concurrency and Computation: Practice and Experience* 22(1):1-14
- Castillo MC, Inagaki A, Kanda M (2011) The effects of inner-and outer-layer turbulence in a convective boundary layer on the near-neutral inertial sublayer over an urban-like surface. *Boundary-Layer Meteorol* 140(3):453-469
- Cheng H, Castro IP (2002) Near wall flow over urban - like roughness. *Boundary-Layer Meteorol* 104(2):229-259
- Coceal O, Belcher SE (2004) A canopy model of mean winds through urban areas. *Q J R Meteorol Soc* 130(599):1349-1372
- Davis FK, Newstein H (1968) The variation of gust factors with mean wind speed and with height. *J App Meteorol* 7(3):372-378
- Garratt JR (1990). The internal boundary layer - a review. *Boundary-Layer Meteorol* 50(1-4):171-203  
Gust. Retrieved from <http://www.merriam-webster.com/dictionary/gust>
- He J, Song CCS (1999) Evaluation of pedestrian winds in urban area by numerical approach. *J Wind Eng* 81:295-309
- He X, Zou Q, Luo LS, Dembo M (1997) Analytic solutions of simple flows and analysis of nonslip boundary conditions for the lattice Boltzmann BGK model. *J Stat Phys* 87(1-2):115-136
- Hou S, Sterling J, Chen S, Doolen GD (1994) A lattice Boltzmann subgrid model for high Reynolds number flows. arXiv preprint comp-gas/9401004
- Hu T, Yoshie R (2013) Indices to evaluate ventilation efficiency in newly-built urban area at pedestrian level. *J Wind Eng Ind Aerodyn* 112:39-51
- Huda AN, Inagaki A, Kanda M, Onodera N, Aoki T (2015) Large eddy simulation of the gust index in an urban area using the lattice Boltzmann method. *Boundary-Layer Meteorol* (Under review)



- Huda AN, Inagaki A, Kanda M, Onodera N, Aoki T (2015) Spatial distribution of the gust index over an urban area in Tokyo. Proceedings of the 9th International Conference on Urban Climate jointly with 12th Symposium on the Urban Environment, 20-24 July, 2015, Toulouse, France
- Huda AN, Inagaki A, Kanda M, Onodera N, Aoki T (2015) Large eddy simulation of the gust factor using lattice Boltzmann method within a huge and high resolution urban area of Tokyo. J Japan Society of Civil Engineers, Ser. B1(Hydraulic Engineering) 71(4):I\_37-I\_42
- Huda AN, Inagaki A, Kanda M, Onodera N, Aoki T (2014) A Huge and high resolution large eddy simulation domain of Tokyo urban area by using lattice Boltzmann method. Proceedings of the Academy for Co-creative Education of Environment and Energy Science, 12-16 December, 2014, Perth, Western Australia, Australia
- Huda AN, Inagaki A, Kanda M, Onodera N, Aoki T (2014) Simulation of the gust factor in highly dense urban area in Tokyo. Proceedings of the 1st International Conference on Computational Engineering and Science for Safety and Environmental Problems, 13-16 April, 2014, SIC, Sendai, Japan, pp 718-72
- Inagaki A, Castillo MCL, Yamashita Y, Kanda M, Takimoto H (2012) Large-eddy simulation of coherent flow structures within a cubical canopy. *Boundary-Layer Meteorol* 142(2):207-222  
Japan Meteorological Agency (JMA), <http://www.jma.go.jp/jma/index.html>
- Jiménez J (2004) Turbulent flows over rough walls. *Annu Rev Fluid Mech* 36:173-196
- Kanda M (2006) Large-eddy simulations on the effects of surface geometry of building arrays on turbulent organized structures. *Boundary-Layer Meteorol* 118(1):151-168
- Kanda M, Inagaki A, Miyamoto T, Gryschka M, Raasch S (2013) A New Aerodynamic Parametrization for Real Urban Surfaces. *Boundary-Layer Meteorol* 148(2):357-377
- Kanda M, Moriwaki R, Kasamatsu F (2004) Large-eddy simulation of turbulent organized structures within and above explicitly resolved cube arrays. *Boundary-Layer Meteorol* 112(2):343-368
- Keck M, Raasch S, Letzel MO, Ng E (2014) First Results of High Resolution Large-Eddy Simulations of the Atmospheric Boundary Layer. *J Heat Island Inst Int* 9(2):39-43
- Kobayashi H, Ham F, Wu X (2008) Application of a local SGS model based on coherent structures to complex geometries. *Int J Heat Fluid Flow* 29(3):640-653
- Kobayashi H (2006) Large eddy simulation of magnetohydrodynamic turbulent channel flows with local subgrid-scale model based on coherent structures. *Phys Fluids (1994-present)* 18(4):045107
- Kubota T, Miura M, Tominaga Y, Mochida A (2008) Wind tunnel tests on the relationship between building density and pedestrian-level wind velocity: Development of guidelines for realizing acceptable wind environment in residential neighborhoods. *Build Environ* 43:1699-1708
- Leonardi S, Castro IP (2010) Channel flow over large cube roughness: a direct numerical simulation study. *J Fluid Mech* 651:519-539
- Letzel MO, Helmke C, Ng E, An X, Lai A, Raasch S (2012) LES case study on pedestrian level ventilation in two neighbourhoods in Hong Kong. *Meteorol Z* 21(6):575-589
- Letzel MO, Krane M, Raasch S (2008) High resolution urban large-eddy simulation studies from street canyon to neighbourhood scale. *Atmos Environ* 42(38):8770-8784

- Macdonald RW (2000) Modelling the mean velocity profile in the urban canopy layer. *Boundary-Layer Meteorol* 97(1):25-45
- Martilli A, Clappier A, Rotach MW (2002) An urban surface exchange parameterisation for mesoscale models. *Boundary-Layer Meteorol* 104(2):261-304
- Martinuzzi R, Tropea C (1993) The flow around surface-mounted, prismatic obstacles placed in a fully developed channel flow (Data Bank Contribution). *J Fluids Eng* 115(1):85-92
- Monahan HH, Armendariz M (1971) Gust factor variations with height and atmospheric stability. *J Geophys Res* 76(24):5807-5818
- Murakami S, Fujii K (1983) Turbulence characteristics of wind flow at ground level in built-up area. *J Wind Eng Ind Aerodyn* 15:133-144
- Nakayama H, Takemi T, Nagai H (2011) LES analysis of the aerodynamic surface properties for turbulent flows over building arrays with various geometries. *J App Meteorol Clim*, 50(8):1692-1712
- National Oceanic and Atmospheric Administration (NOAA), <http://www.noaa.gov/>
- Oke TR (1987) *Boundary layer climates*. 2nd edn. Methuen, London 435 pp
- Onodera N, Aoki T, Shimokawabe T, Kobayashi H (2013) Large-scale LES wind simulation using lattice Boltzmann method for a 10km × 10km area in metropolitan Tokyo. *TSUBAME e-Science J Global Sci Inf Comput Cent* 9:1-8
- Park SB, Baik JJ, Han BS (2013) Large-eddy simulation of turbulent flow in a densely built-up urban area. *Environ Fluid Mech* 15(2):235-250
- Raasch S, Schröter M (2001) PALM – A large-eddy simulation model performing on massively parallel computers. *Meteorol Z* 10:363-372
- Raupach MR, Antonia RA, Rajagopalan S (1991). Rough-wall turbulent boundary layers. *App Mech Rev* 44(1):1-25
- Razak AA, Hagishima A, Ikegaya N, Tanimoto J (2013) Analysis of airflow over building arrays for assessment of urban wind environment. *Build Environ* 59:56-65
- Roth M (2000) Review of atmospheric turbulence over cities. *Q J R Meteorol Soc* 126(564):941-990
- Takebayashi H, Oku K (2014) Study on the evaluation method of wind environment in the street canyon for the preparation of urban climate map. *J Heat Island Inst Int* 9(2):55-60
- Verkaik JW (2000) Evaluation of two gustiness models for exposure correction calculations. *J Appl Meteorol* 39(9):1613-1626
- Wieringa J (1973) Gust factors over open water and built-up country. *Boundary-Layer Meteorol* 3(4):424-441
- Wilson DK (2000) *The Role of Wind Gusts in the Near-Ground Atmosphere* (No. ARL-TR-2290). Army Res Lab Adelphi MD 51 pp
- Wind gust. Retrieved from <http://graphical.weather.gov/definitions/defineWindGust.html>
- Xie ZT, Coceal O, Castro IP (2008) Large-eddy simulation of flows over random urban-like obstacles. *Boundary-Layer Meteorol* 129(1):1-23
- Yin X, Zhang J (2012) An improved bounce-back scheme for complex boundary conditions in lattice Boltzmann method. *J Comput Phys* 231(11):4295-4303

- Yu H, Girimaji SS, Luo LS (2005) DNS and LES of decaying isotropic turbulence with and without frame rotation using lattice Boltzmann method. *J Comput Phys* 209(2):599–61
- Zaki SA, Hagishima A, Tanimoto J, Ikegaya, N (2011) Aerodynamic parameters of urban building arrays with random geometries. *Boundary-Layer Meteorol* 138(1): 99-120
- Zou Q, He X (1996) On pressure and velocity flow boundary conditions and bounce back for the lattice Boltzmann BGK model. eprint. arXiv preprint comp-gas/9611001